PHYSICAL REVIEW D **73,** 063008 (2006)

Accessibility of the pre-big-bang models to LIGO

Vuk Mandic
LIGO Laboratory, California Institute of Technology, MS 18-34, Pasadena, California 91125, USA

Alessandra Buonanno
Department of Physics, University of Maryland, College Park, Maryland 20742, USA
AstroParticule et Cosmologie (APC) 11, place Marcelin Berthelot, 75005 Paris, France*
(Received 12 October 2005; published 17 March 2006)

The recent search for a stochastic background of gravitational waves with LIGO interferometers has produced a new upper bound on the amplitude of this background in the 100 Hz region. We investigate the implications of the current and future LIGO results on pre-big-bang models of the early Universe, determining the exclusion regions in the parameter space of the minimal pre-big-bang scenario. Although the current LIGO reach is still weaker than the indirect bound from big bang nucleosynthesis, future runs by LIGO, in the coming year, and by Advanced LIGO (~ 2009) should further constrain the parameter space, and in some parts surpass the Big Bang nucleosynthesis bound. It will be more difficult to constrain the parameter space in nonminimal pre-big bang models, which are characterized by multiple cosmological phases in the yet not well understood stringy phase, and where the higher-order curvature and/or quantum-loop corrections in the string effective action should be included.

DOI: 10.1103/PhysRevD.73.063008 PACS numbers: 95.85.Sz, 04.80.Nn, 98.70.Vc, 98.80.Cq

I. INTRODUCTION

The Laser Interferometer Gravitational-wave Observatory (LIGO) has built three multikilometer interferometers, designed to search for gravitational waves (GWs). One of the possible targets of such a search is the stochastic background of gravitational waves. Many possible sources of such a background have been proposed (see, e.g., [1–3] for reviews). Some of these sources are astrophysical in nature, such as rotating neutron stars, supernovae or low-mass X-ray binaries. Others are cosmological, such as the amplification of quantum-vacuum fluctuations during inflation [4,5], phase transitions [6], and cosmic strings [7]. Most of these sources are expected to be very weak and below the sensitivity of the LIGO interferometers. Furthermore, they are constrained by several observations.

The measurement of the cosmic microwave background by the Cosmic Background Explorer (COBE) bounds the logarithmic spectrum of gravitational waves [8] to $\Omega_{\rm GW}(f)h_{100}^2 < 8 \times 10^{-14}$ at $\sim 10^{-16}$ Hz [9], where $h_{100} = H_0/(100\ {\rm km/s/Mpc}) \approx 0.72$ is the ''reduced'' Hubble parameter [10]. Since in standard (slow-roll) inflationary models, the spectrum produced by the parametric amplification of quantum-vacuum fluctuations [4] is expected to be (almost) flat at higher frequencies [11], a similar bound applies at higher frequencies, as well. In some inflationary models in which a cosmological phase with equation of state stiffer than radiation comes before the radiation era, the spectrum at high frequency could increase as function of frequency, thus avoiding the COBE bound. For example this happens in quintessential inflation [12]. The GW spectrum could mildly increase as function of frequency in scenarios in which inflation occurs with an equation of state $w < -1$ [13]—some examples are given in Ref. [14] where inflation is obtained from a noncanonical Lagrangian. In other scenarios of superstring cosmology, as the cyclic/ekpyrotic models [15], the GW spectrum also increases as function of frequency, but its normalization makes it unobservable by ground- and space-based detectors.

The arrival times of the millisecond pulsars can be used to place a bound at $\sim 10^{-8}$ Hz [16]: $\Omega_{\rm GW}(f)h_{100}^2 < 9.3 \times 10^{-8}$. Doppler tracking of the Cassini spacecraft can be used to arrive at yet another bound, in the 10^{-6}–10^{-3} Hz band [17]: $\Omega_{\rm GW}(f)h_{100}^2 < 0.014$. The big bang nucleosynthesis (BBN) model and observations can be used to constrain the integral of the GW spectrum $\int \Omega_{\rm GW}h_{100}^2 d(\ln f) < 6.3 \times 10^{-6}$ [1,2,18]. Finally, the ground-based interferometers and resonant bars can probe the spectrum of gravitational waves in the band 10 Hz—few kHz. The most recent bound from LIGO is $\Omega_{\rm GW}h_{100}^2 < 4.2 \times 10^{-4}$ for a flat spectrum in the 69–156 Hz band [19].

In this paper, we focus on the implications of the recent LIGO result on pre-big bang (PBB) models [20], and we investigate their accessibility to future LIGO searches. The PBB models predict a stochastic GW spectrum whose amplitude can increase as a function of frequency in some frequency ranges. Hence, they can avoid the bounds due to the CMB, pulsar timing, and Doppler tracking, and predict relatively large background in the frequency band where LIGO is sensitive. In Sec. II we briefly review the GW spectrum in the minimal PBB models. In Sec. III we discuss the latest result from the LIGO search for the stochastic GW background. In Sec. IV we study how the

*UMR 7164 (CNRS, Université Paris 7, CEA, Observatoire de Paris)

new LIGO results, and the expected future results, constrain the free parameters of the minimal PBB models. In Sec. V we discuss how modifications of the minimal PBB model can affect the observability of the stochastic GW background. Finally, we conclude in Sec. VI.

II. THE GRAVITATIONAL WAVE SPECTRUM IN THE MINIMAL PRE-BIG-BANG MODEL

In the PBB scenario (see, e.g., [20–23]), the initial state of the Universe is assumed to be the string perturbative vacuum, where the Universe can be described by the low-energy string effective action. The kinetic energy of the dilaton field drives the Universe through an inflationary evolution (henceforth denoted dilaton-inflationary phase), which is an accelerated expansion in the string frame, or accelerated contraction (gravitational collapse) in the (usual) Einstein frame. The spacetime curvature increases in the dilaton-inflationary phase, eventually reaching the order of the string scale. At this point, the low-energy string effective action is no longer an accurate description of the Universe, and higher-order corrections (higher-curvature and/or quantum-loop corrections) should be included in the string action. These corrections are expected to reduce or stop the growth of the curvature, *removing* the would-be big bang singularity. The exact evolution of the Universe in this high curvature and/or strong-coupling phase (henceforth denoted by *stringy* phase) is currently not known [20]. The end of the stringy phase is what one could refer to as the ''big bang''—the Universe's transition into the radiation phase, which is then followed by the matter-dominated and acceleration-dominated phases.

Although the transition between the inflationary PBB phase and the post-big bang phase is not well understood, some models have been proposed in the literature which can partially describe it. In the following, we focus on the model derived in Ref. [24] where, in the string frame, the dilaton-inflationary phase is followed by a phase of constant curvature with the dilaton field growing linearly in time. It is then assumed that at the end of this stringy phase the dilaton reaches the present vacuum expectation value and stops. This model has been denoted in the literature as the ''minimal'' PBB model. Within this model, the stochastic GW background has been evaluated [25–27]. For simplicity, in this paper we use the result for the logarithmic spectrum of gravitational waves [4] as evaluated in Ref. [27]:

$$h_{100}^2\Omega_{\rm GW}(f) = b(\mu)\frac{(2\pi f_s)^4}{H_{100}^2 M_{\rm Pl}^2}\left(\frac{f_1}{f_s}\right)^{2\mu+1}\left(\frac{f}{f_s}\right)^{5-2\mu} \times \left| H_0^{(2)}\left(\frac{\alpha f}{f_s}\right)J'_\mu\left(\frac{f}{f_s}\right) + H_1^{(2)}\left(\frac{\alpha f}{f_s}\right)J_\mu\left(\frac{f}{f_s}\right) - \frac{(1-\alpha)}{2\alpha}\frac{f_s}{f}H_0^{(2)}\left(\frac{\alpha f}{f_s}\right)J_\mu\left(\frac{f}{f_s}\right)\right|^2, \quad (1)$$

$$b(\mu) = \frac{\alpha}{48}2^{2\mu}(2\mu-1)^2\Gamma^2(\mu), \qquad \alpha = \frac{1}{1+\sqrt{3}},$$

where $H_{0,1}^{(2)}$, J_μ, and Γ are the Hankel, Bessel and Gamma functions, respectively, $H_{100} = 100$ km/s/Mpc, and $M_{\rm Pl}$ is the Planck mass; f_s is the GW frequency redshifted until today of fluctuations exiting the Hubble radius at the time of the transition between the dilaton and the stringy phase; μ is a dimensionless free parameter that measures the growth of the dilaton during the stringy phase, effectively determining the slope of the spectrum in the high-frequency limit (see below). The low-frequency limit of Eq. (1) is given by [27]:

$$h_{100}^2\Omega_{\rm GW}(f) \simeq \frac{(2\mu-1)^2}{192\mu^2\alpha}\frac{(2\pi f_s)^4}{H_{100}^2M_{\rm Pl}^2}\left(\frac{f_1}{f_s}\right)^{2\mu+1}\left(\frac{f}{f_s}\right)^3 \times\left\{(2\mu\alpha-1+\alpha)^2+\frac{4}{\pi^2}\left[(2\mu\alpha-1+\alpha)\times\left(\ln\frac{\alpha f}{2f_s}+\gamma_E\right)-2\right]^2\right\}, \quad \gamma_E = 0.5772, \quad (2)$$

while the high-frequency limit is [27]:

$$h_{100}^2\Omega_{\rm GW}(f) \simeq \frac{4b(\mu)}{\pi^2\alpha}\frac{(2\pi f_1)^4}{H_{100}^2M_{\rm Pl}^2}\left(\frac{f}{f_1}\right)^{3-2\mu}. \quad (3)$$

The parameter f_1 appearing in the above equations is the GW frequency redshifted until today of fluctuations exiting the Hubble radius when the stringy phase ends. This is the largest frequency (smallest scale) for which fluctuations are amplified—hence, f_1 is also the high-frequency cutoff of the GW spectrum.

Thus, the GW spectrum in the minimal PBB scenario increases as f^3 for $f \ll f_s$, goes as $f^{3-2\mu}$ for $f_s \ll f \ll f_1$, and vanishes exponentially for $f > f_1$. An example of such a spectrum is shown in Fig. 3 of Ref. [27], and we reproduce it in Fig. 1.

Let us now focus on the free parameters of the model. The parameter μ is, by definition, limited to positive values. We will only consider the case $\mu \leq 1.5$—for $\mu > 1.5$ the decreasing spectrum would easily violate the existing experimental bounds [27]. The parameter f_s varies over the range $0 < f_s < f_1$. Since the spectrum sharply decreases for frequencies below f_s, LIGO's reach for models where f_s is above the LIGO band quickly diminishes. In particular, to avoid the f^3 dependence in the LIGO frequency band, $f_s \lesssim 30$ Hz is necessary. Furthermore, Eq. (3) shows that in the high-frequency limit the spectrum does not depend on f_s. Hence, if $f_s \lesssim 30$ Hz, it does not matter what it is, as far as the accessibility to LIGO is concerned. Finally, the parameter f_1 can be approximated as [27,28]:

$$f_1 \simeq 4.3\times10^{10}\ {\rm Hz}\left(\frac{H_s}{0.15M_{\rm Pl}}\right)\left(\frac{t_1}{\lambda_s}\right)^{1/2}, \quad (4)$$

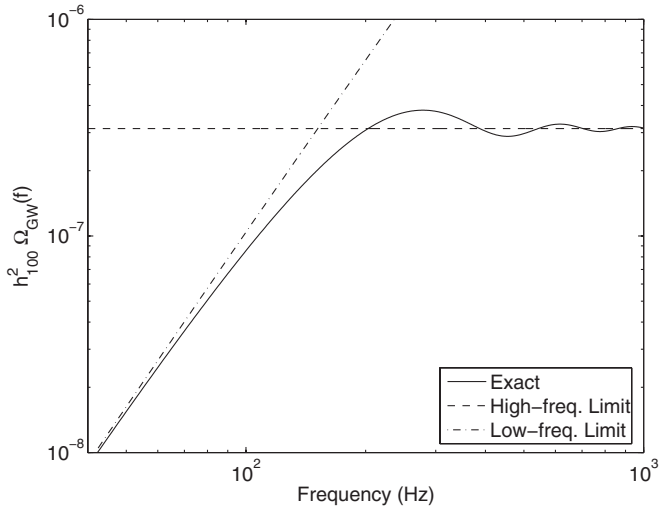

FIG. 1. $h_{100}^2\Omega_{\rm GW}(f)$ vs f, as predicted by the PBB model with $f_s = 100$ Hz, $f_1 = 4.3 \times 10^{10}$ Hz, and $\mu = 1.5$.

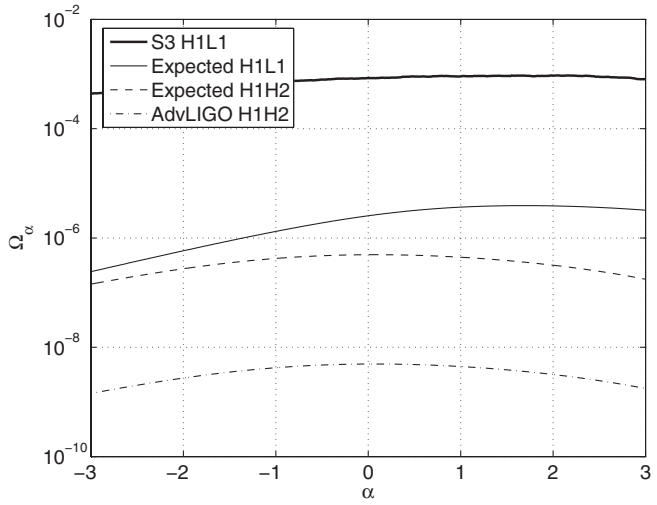

FIG. 2. The 90% UL on Ω_α is shown as a function of the spectral slope α for the most recent LIGO result. Expected sensitivities of LIGO and of Advanced LIGO are also shown.

where H_s is the (constant) Hubble parameter during the stringy phase, t_1 is the time when the string phase ends, and λ_s is the string length. The values $H_s \approx 0.15 M_{\rm Pl}$ and $t_1 \approx \lambda_s$ are the most natural ones [27,29], but they might vary by an order of magnitude. Since $\Omega_{\rm GW}(f) \sim f_1^4$ [see Eq. (3)], this variation leads to a very large variation in the amplitude of the GW spectrum. Hence, although the theoretically predicted value for f_1 is more robust than those for f_s and μ, we shall explore the possibility of varying f_1 around its most natural value [30].

III. SEARCHING FOR STOCHASTIC GRAVITATIONAL WAVES WITH LIGO

The method of searching for stochastic gravitational waves with interferometers has been studied by many authors [32–34]. Following Allen and Romano [34], we can define the following cross-correlation estimator:

$$Y = \int_{-\infty}^{+\infty} Y(f) df = \int_{-\infty}^{+\infty} df \int_{-\infty}^{+\infty} df' \delta_T(f - f') \tilde{s}_1(f)^* \tilde{s}_2(f') \tilde{Q}(f'), \quad (5)$$

where δ_T is a finite-time approximation to the Delta function, $\tilde{s}_1$ and $\tilde{s}_2$ are the Fourier transforms of the strain time-series of two interferometers, and $\tilde{Q}$ is the optimal filter. Assuming that the detector noise is Gaussian, stationary, uncorrelated between the two interferometers, and uncorrelated with and much larger than the GW signal, the variance of the estimator Y is given by:

$$\sigma_Y^2 \approx \frac{T}{2} \int_0^{+\infty} df P_1(f) P_2(f) \mid \tilde{Q}(f)|^2, \quad (6)$$

where $P_i(f)$ are the power spectral densities of the two interferometers, and T is the measurement time. Finally, it can be shown that the optimal filter can be written in the form [34]:

$$\tilde{Q}(f) = N \frac{\gamma(f) \Omega_t(f)}{f^3 P_1(f) P_2(f)}, \quad (7)$$

where $\gamma(f)$ is the overlap reduction function (arising from the different locations and orientations of the two interferometers), and $\Omega_t(f)$ is the template spectrum to be searched. Assuming the template spectrum $\Omega_t(f) = \Omega_\alpha (f/100\ {\rm Hz})^\alpha$, the normalization constant N can be chosen such that $\langle Y \rangle = \Omega_\alpha T$.

This analysis procedure was implemented in the recent analysis of the LIGO data, using the 4 km interferometers at Hanford, WA and Livingston, LA, for the science run S3 [19]. This analysis yielded the 90% upper limit of $\Omega_0 < 8.4 \times 10^{-4}$ for the flat template spectrum $\Omega_t(f) = \Omega_0$. Once $Y(f)$ is estimated for the flat spectrum, one can apply simple scaling by the appropriate power law to obtain the estimates for different values of α (similar procedure can be followed for an arbitrary spectral shape). Figure 2 shows the 90% UL on Ω_α as a function of the spectral slope α for the S3 run, as well as the expected reach for LIGO and for Advanced LIGO. Here and in the following by expected LIGO (H1L1 and H1H2) we mean LIGO design sensitivity and 1 yr of observation, and by Advanced LIGO we assume a sensitivity 10 times better than the LIGO design and 1 yr of observation. [LIGO has started the year-long run at design sensitivity in November 2005.]

IV. SCANNING THE PARAMETER SPACE

We now study the accessibility of the minimal PBB model discussed in Sec. II to the most recent and future runs of LIGO, and to Advanced LIGO. Previous investigations, which did not use real data, were done in Refs. [35,36].

As discussed in Sec. II, the amplitude of the GW spectrum in the PBB models is proportional to f^3 at frequencies below f_s. Hence, the sensitivity of LIGO to PBB models decreases as f_s is increased. To avoid the f^3 dependence of the spectrum in the LIGO frequency band, we choose $f_s = 30$ Hz. For such choice of f_s, the LIGO band falls in the relatively flat part of the GW spectrum. We vary f_1 by a factor of 10 around the most natural value estimated in Eq. (4) (i.e., between 4.3×10^9 and 4.3×10^{11}) and we vary μ between 1 and 1.5 (models with $\mu < 1$ are out of reach of LIGO, as shown below). For each point in the $\mu - f_1$ plane, we evaluate $\Omega_\alpha = \Omega_{\rm GW}(f = 100\ {\rm Hz})$ predicted by the model, and we check whether it is excluded by the experimental (or future expected) results. We also integrate the predicted spectrum and check whether it passes the BBN bound [1,2,18]:

$$\int \Omega_{\rm GW}(f) h_{100}^2 d(\ln f) < 6.3 \times 10^{-6}, \qquad (8)$$

assuming the number of neutrino species $N_\nu < 3.9$ [27,37]. We use $h_{100} = 0.72$ as the reduced Hubble parameter [10]. Figure 3 shows the 90% UL exclusion curves obtained in this way. The latest result from LIGO (S3 run) is just beginning to probe this parameter space. The future runs of LIGO (and of Advanced LIGO) are expected to probe a more significant part of the parameter space, becoming comparable to or even surpassing the BBN bound. As expected, LIGO is most sensitive to models with $\mu = 1.5$, which corresponds to the flat spectrum at high frequencies. As μ decreases from 1.5, the spectral slope increases, and the spectrum in the LIGO band drops quickly below LIGO sensitivity. Although the BBN bound also weakens for $\mu < 1.5$, the effect is not as dramatic because this bound is placed on the integral of the spectrum over a large frequency range. Note that the LIGO S3 run is sensitive to PBB models with $f_1 \geq 2.7 \times 10^{11}$ Hz, relatively large compared to the most natural value estimated in Eq. (4). This is true independent of f_s: for $f_s < 30$ Hz, Fig. 3 would not change, while for $f_s > 30$ Hz all bounds would weaken. Finally, the Advanced LIGO is expected to reach models with the most natural value of $f_1 = 4.3 \times 10^{10}$ Hz.

It is also possible to use Eq. (4) to turn a bound on f_1 into an exclusion curve in the t_1/λ_s vs $H_s/(0.15 M_{Pl})$ plane. In this way, the GW experiments can be used to constrain string-related parameters in the framework of the PBB model. As an example, we choose $\mu = 1.5$ and $f_s = 30$ Hz as the optimal case for LIGO, and determine the 90% UL exclusion curves for different experiments. These curves are shown in Fig. 4. Again, the latest LIGO result is weaker than the BBN bound, but the future LIGO and Advanced LIGO searches are expected to explore a larger, more physical part of this parameter space.

One can also examine the accessibility of the models in the $f_s - \mu$ plane. For the relatively large value $f_1 = 4.3 \times 10^{11}$ Hz, which makes the model's stochastic GW back-

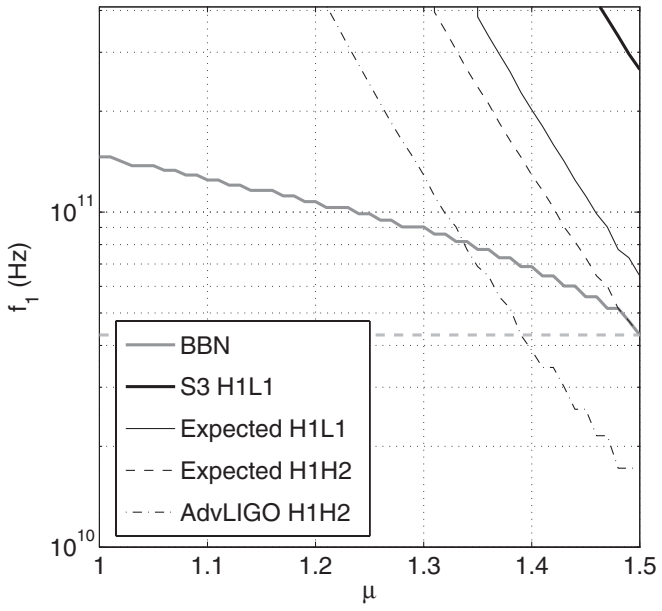

FIG. 3. The 90% UL exclusion curves are shown in the $f_1 - \mu$ plane for $f_s = 30$ Hz (the excluded regions are above the corresponding curves). We show the latest result from LIGO, and the future expected reach of LIGO and of Advanced LIGO. The limit from the BBN is also shown. The horizontal gray dashed line denotes the most natural value of f_1, given by Eq. (4).

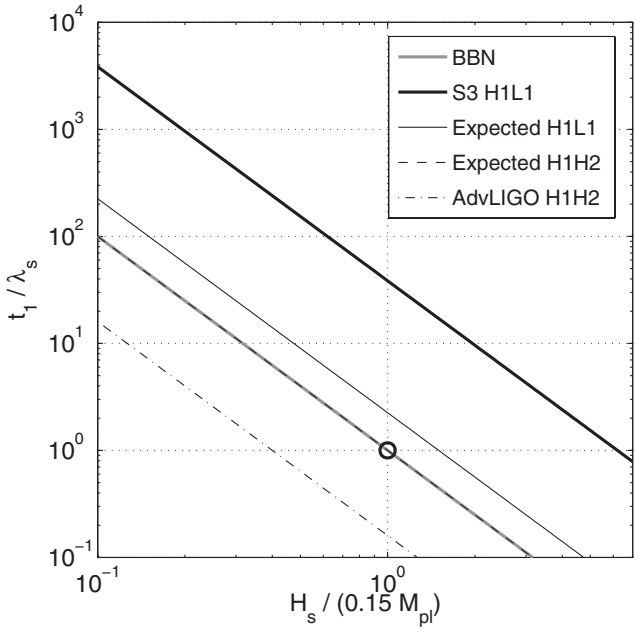

FIG. 4. The 90% UL exclusion curves are shown in the t_1/λ_s vs $H_s/(0.15 M_{\rm Pl})$ plane, for $\mu = 1.5$ and $f_s = 30$ Hz (the excluded regions are above the corresponding curves). We show the latest result from LIGO, and the future expected reach of LIGO and of Advanced LIGO. The limit from the BBN is also shown. The black circle denotes the most natural point, as given in Eq. (4).

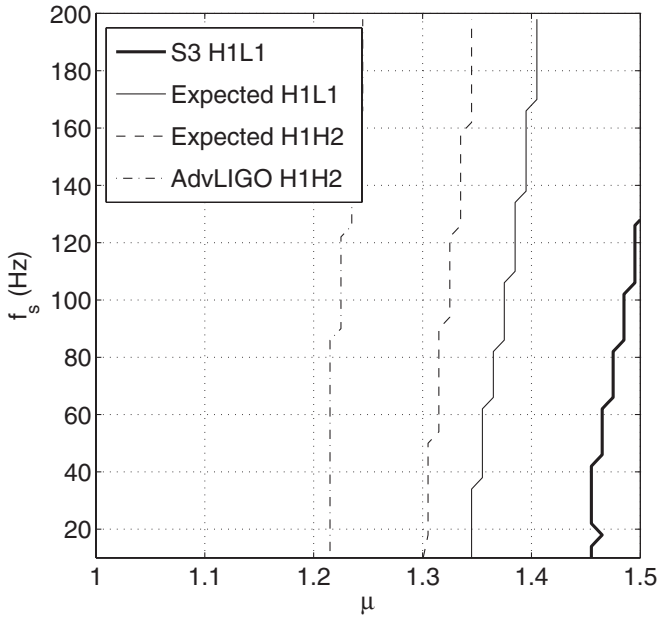

FIG. 5. The 90% UL exclusion curves are shown in the $f_s - \mu$ plane, for $f_1 = 4.3 \times 10^{11}$ Hz (the excluded regions are to the right from the corresponding curves). We show the latest result from LIGO, and the future expected reach of LIGO and of Advanced LIGO. The indirect limit from the BBN excludes the whole region shown in this plane.

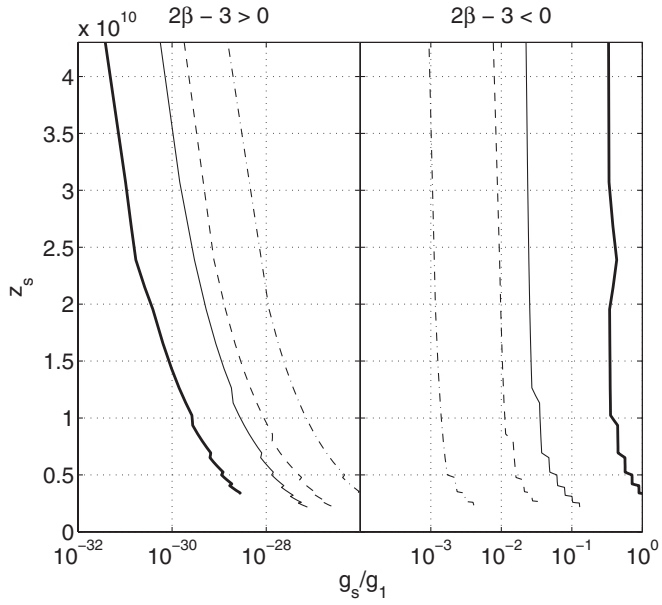

FIG. 6. The 90% UL exclusion curves are shown in the $z_s - g_s$ plane, for $f_1 = 4.3 \times 10^{11}$ Hz. We show the latest result from LIGO (thick solid), and the future expected reach of LIGO (thin solid for the H1L1 pair, dashed for the H1H2 pair) and of Advanced LIGO (dash-dotted). The two sets of curves correspond to positive (left) and negative (right) signs of $(2\beta - 3)$.

ground accessible to the LIGO S3 run, we performed a scan in the $f_s - \mu$ plane. Figure 5 shows the results. Note that for the flat spectrum ($\mu = 1.5$), the S3 run of LIGO is sensitive to models with $f_s \lesssim 120$ Hz; future runs of LIGO and Advanced LIGO are expected to probe higher values of f_s as well. Also note that the exclusion curves in Fig. 5 are almost vertical (i.e. not very sensitive to f_s). This is a consequence of the large value of f_1—for smaller values of f_1, the accessibility of models to LIGO would depend more strongly on the value of f_s.

Several papers in the literature [25,26,38], parametrize the GW spectrum in the minimal PBB model in terms of $z_s = f_1/f_s$ and g_s, defined by $g_s/g_1 = (f_s/f_1)^\beta$, with β given by $2\mu = |2\beta - 3|$. The parameter z_s is the total redshift during the stringy phase, thus it quantifies its duration, while g_1 and g_s are the string couplings at the end and at the beginning of the stringy phase, respectively. Figure 6 shows the curves from Fig. 5 converted into the $z_s - g_s$ plane, using $f_1 = 4.3 \times 10^{11}$ Hz, and setting g_1 to its most natural value given by $g_1^2/(4\pi) = \alpha_{\rm GUT}$.

V. GOING BEYOND THE MINIMAL PRE-BIG-BANG MODEL

In this section we investigate how extensions of the minimal PBB model or variations of it can impact the accessibility of the stochastic GW background to LIGO and to Advanced LIGO.

The GW spectrum in the minimal PBB model was originally evaluated [25–27] neglecting the higher-curvature corrections in the equation of tensorial fluctuations during the stringy phase. Gasperini [39] evaluated the higher-order equation for tensorial fluctuations and showed that these corrections modify the amplitude of the perturbation *only* by a factor of order one. Hence, these corrections are not expected to affect our results significantly.

In Refs. [38,40] the authors have examined the effect of radiation production via some reheating process occuring below the string scale. Such a process may be needed to dilute several relic particles produced during (or at the very end of) the PBB phase, whose abundance could spoil the BBN predictions [41]. Depending on when and for how long the entropy production occurs, it can change both the shape and the amplitude of the GW spectrum in the frequency region around 100 Hz. In general, the amplitude of the spectrum at these frequencies is reduced. If we assume that the reheating process occurs at the end of the stringy phase (i.e., all of the entropy is produced at the end of the stringy phase), then the effect of the process is a simple scaling of the original spectrum by the factor $(1 - \delta s)^{4/3}$, where δs is the fraction of the present thermal entropy density that was produced in the process. Figure 7 shows the exclusion curves in the $f_s - \mu$ plane for $\delta s = 0.5$. By comparing to Fig. 5, we can see that the effect weakens all bounds.

Another possible, but somewhat arbitrary variation of the model, was examined by Allen and Brustein [35]. They

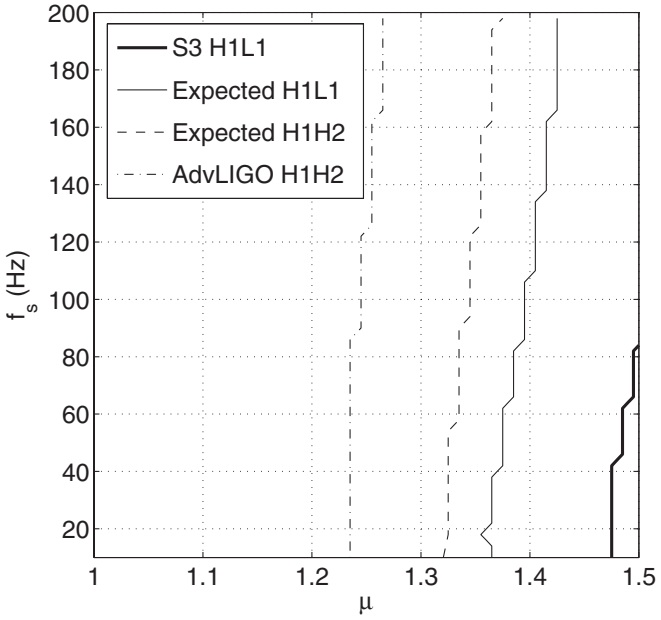

FIG. 7. The 90% UL exclusion curves are shown in the $f_s - \mu$ plane for $f_1 = 4.3 \times 10^{11}$ Hz and for $\delta s = 0.5$ (the excluded regions are to the right of the corresponding curves). We show the latest result from LIGO, and the future expected reach of LIGO and of Advanced LIGO. The indirect BBN limit excludes all models shown in this plane.

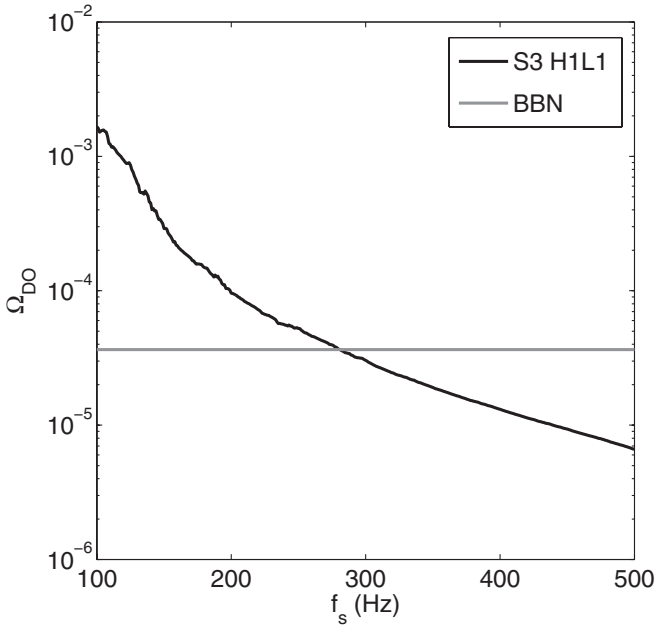

FIG. 8. The 90% UL on $\Omega_{\rm DO}$ is shown as a function of f_s for the models where stochastic gravitational background is not produced during the string phase. The latest LIGO result and the BBN bound are shown.

assumed that stochastic gravitational waves are not produced during the stringy phase, but only during the dilaton phase. This is achieved by setting $f_1 = f_s$ and assuming that $\Omega_{\rm GW}$ vanishes for $f_s < f$. Such a model is not well motivated in the PBB scenario, but it is phenomenologically interesting as it represents a class of models whose spectrum peaks in the LIGO band. The spectrum of this model can, therefore, be approximated by:

$$\Omega_{\rm GW}(f) = \begin{cases} \Omega_{\rm DO}\left(\frac{f}{f_s}\right)^3 & f < f_s, \\ 0 & f > f_s. \end{cases} \qquad (9)$$

The BBN bound becomes weaker because the integral in Eq. (8) is performed over a much smaller frequency range, and it can be written as $\Omega_{\rm DO} < 3.8 \times 10^{-5}$. Figure 8 shows the bound from the latest LIGO result as a function of f_s. Note that this bound is already better than the BBN bound for $f \gtrsim 300$ Hz.

Finally, as first noticed in Ref. [40], it is well possible that many more cosmological phases are present between the pre- and the post-big bang eras—some examples are given in Refs. [40,31]. If this is the case, the GW spectra during the high-curvature and/or strong-coupling region will be characterized by several branches with increasing and decreasing slopes. Because of the dependence of the spectra on a larger number of parameters, it would be more difficult to constrain these nonminimal scenarios, even when LIGO overcomes the BBN bound.

VI. CONCLUSIONS

Using the most recent LIGO search for the stochastic gravitational background [19], we determined the exclusion regions in the parameter space of the PBB minimal model [20]. We found that the most recent S3 run can access the stochastic GW background only if f_1 is larger than the most natural value 4.3×10^{10} Hz (i.e. only if $f_1 > 2.7 \times 10^{11}$ Hz; see Fig. 3). In this case the S3 run of LIGO can exclude the region in the (f_s, μ) parameter space with $\mu \approx 1.5$ (i.e., almost a flat spectrum) and $f_s \lesssim 120$ Hz (see Fig. 5). A one-year run of LIGO at the design sensitivity will be able to start excluding regions with sligthly increasing GW spectrum (as a function of frequency), while Advanced LIGO could exclude spectra with slopes of at most ≈ 0.5. Models with larger values of f_s will become accessible, as well as with lower values of f_1, including the most natural value $f_1 = 4.3 \times 10^{10}$ Hz.

As shown in Fig. 3, the BBN bound already *excludes* all models accessible to the LIGO S3 run. However, it should be noted that: (i) the LIGO S3 bound is a result of a direct measurement of the stochastic background of gravitational waves while BBN bound is not, and (ii) future searches by LIGO and by Advanced LIGO are expected to approach and even surpass (in some parts of the parameter space) the BBN bound.

Analysis of the search in the parameter space more commonly used in the literature (see Fig. 6) shows that LIGO and Advanced LIGO can bound the duration of the stringy phase and the string coupling at the beginning (end) of the stringy phase (dilaton-inflationary phase). Similarly,

as shown in Fig. 4, by constraining f_1 these experiments can constrain other string-related parameters, such as H_s (the Hubble parameter during the stringy phase) and t_1/λ_s (the ratio of the end-time of the stringy phase and of the string length) or the value of the string coupling at the end of the stringy phase g_1.

As emphasized above, the stringy phase is not well understood, yet. Many variations to the minimal PBB model analyzed in this paper are possible and have been proposed [38,40,31]. They can significantly change the shape and the amplitude of the spectrum in the frequency range around 100 Hz, hence improving or reducing the accessibility of the PBB models to LIGO. The presence of multi cosmological phases [40] during the stringy phase will make much harder the determination of the exclusion regions in the PBB parameter space. More robust predictions for the stringy phase would be strongly desirable.

ACKNOWLEDGMENTS

The authors thank Albert Lazzarini, Joe Romano, and Stan Whitcomb for many useful discussions, Maurizio Gasperini for useful comments, and the LIGO Scientific Collaboration for making this study possible. V. M.'s work was supported by the NSF Cooperative Agreement No. PHY-0107417.

[1] M. Maggiore, Phys. Rep. **331**, 283 (2000).
[2] B. Allen, Lectures at Les Houches School (unpublished).
[3] A. Buonanno, *Lectures on Gravitational Waves from the Early Universe*, TASI (unpublished).
[4] L. P. Grishchuk, Sov. Phys. JETP **40**, 409 (1975); Classical Quantum Gravity **10**, 2449 (1993); **14**, 1445 (1997).
[5] A. A. Starobinskii, JETP Lett. **30**, 682 (1979).
[6] A. Kosowsky, M. S. Turner, and R. Watkins, Phys. Rev. D **45**, 4514 (1992); Phys. Rev. Lett. **69**, 2026 (1992); A. Kosowsky and M. S. Turner, Phys. Rev. D **47**, 4372 (1993); M. Kamionkowski, A. Kosowsky, and M. S. Turner, Phys. Rev. D **49**, 2837 (1994); R. Apreda, M. Maggiore, A. Nicolis, and A. Riotto, Nucl. Phys. **B631**, 342 (2002).
[7] R. R. Caldwell and B. Allen, Phys. Rev. D **45**, 3447 (1992); R. R. Caldwell, R. A. Battye, and E. P. S. Shellard, Phys. Rev. D **54**, 7146 (1996); T. Damour and A. Vilenkin, Phys. Rev. Lett. **85**, 3761 (2000); Phys. Rev. D **64**, 064008 (2001).
[8] Note that $\Omega_{\rm GW}$ here should not be confused with the ratio of the total energy density stored in gravitational waves and the critical density of the Universe, i.e., $\Omega_g = \rho_{\rm GW}/\rho_c$. The quantity $\Omega_{\rm GW}$ is the so-called GW spectrum per unit log of frequency: $\Omega_{\rm GW} \equiv (1/\rho_c) d\rho_{\rm GW}/d\log f$. It would have been more appropriate to denote the GW spectrum by $d\Omega_{\rm GW}/d\log f$ and not $\Omega_{\rm GW}$.
[9] B. Allen and S. Koranda, Phys. Rev. D **50**, 3713 (1994).
[10] C. L. Bennet *et al.*, Astrophys. J. Suppl. Ser. **148**, 1 (2003).
[11] M. S. Turner, Phys. Rev. D **55**, R435 (1997); T. L. Smith, M. Kamionkowsky, and A. Cooray, Phys. Rev. D **73**, 023504 (2006); L. A. Boyle, P. Steinhardt, and N. Turok, astro-ph/0507455.
[12] P. J. E. Peebles and A. Vilenkin, Phys. Rev. D **59**, 063505 (1999); M. Giovannini, Phys. Rev. D **60**, 123511 (1999).
[13] L. Grishchuk, Mon. Not. R. Astron. Soc. **360**, 816 (2005).
[14] M. Baldi, F. Finelli, and S. Matarrese, Phys. Rev. D **72**, 083504 (2005).
[15] L. A. Boyle, P. Steinhardt, and N. Turok, Phys. Rev. D **69**, 127302 (2004).
[16] M. P. McHugh *et al.*, Phys. Rev. D **54**, 5993 (1996).
[17] J. W. Armstrong *et al.*, Astrophys. J. **599**, 806 (2003).
[18] E. Kolb and R. Turner, *The Early Universe* (Addison-Wesley, Reading, MA, 1990).
[19] B. Abbot *et al.*, Phys. Rev. Lett. **95**, 221101 (2005).
[20] M. Gasperini and G. Veneziano, Phys. Rep. **373**, 1 (2003).
[21] M. Gasperini and G. Veneziano, Astropart. Phys. **1**, 317 (1993).
[22] M. Gasperini and G. Veneziano, Mod. Phys. Lett. A **8**, 3701 (1993).
[23] M. Gasperini and G. Veneziano, Phys. Rev. D **50**, 2519 (1994).
[24] M. Gasperini, M. Maggiore, and G. Veneziano, Nucl. Phys. **B494**, 315 (1997).
[25] R. Brustein, M. Gasperini, M. Giovannini, and G. Veneziano, Phys. Lett. B **361**, 45 (1995).
[26] R. Brustein, hep-th/9604159.
[27] A. Buonanno, M. Maggiore, and C. Ungarelli, Phys. Rev. D **55**, 3330 (1997).
[28] Note that in evaluating this equation and also the GW spectrum above, we did not include the very recent phase of acceleration of the Universe, but limited to radiation and matter eras. We expect that if the acceleration era were included, the effect on the results presented here would be mild.
[29] The most natural value for H_s was obtained in Ref. [27] by assuming $H_s \sim 1/\lambda_s$ and $\lambda_s^2 \sim (2/\alpha_{\rm GUT}) L_{\rm Pl}^2$ with $\alpha_{\rm GUT} \sim 1/20$.
[30] We note that in the more common version of the minimal PBB model [20,25,31], the frequency f_1 is obtained by imposing that the energy density becomes critical at the beginning of the radiation phase and that the photons we observe today originated from the amplified vacuum fluctuations during the dilaton-driven inflationary phase. Within these assumptions Eq. (4) can be rewritten as $f_1 \simeq g_1^{1/2} (H_s/(0.15 M_{\rm Pl}))^{1/2} (H_0 M_{\rm Pl})^{1/2} \Omega_\gamma^{1/4}$, where $\Omega_\gamma = 4 \times 10^{-5} h_{100}^{-2}$ and g_1 is the string coupling at the end of the stringy phase.
[31] A. Buonanno, K. Meissner, C. Ungarelli, and G. Veneziano, J. High Energy Phys. 01 (1998) 004.
[32] N. Christensen, Phys. Rev. D **46**, 5250 (1992).
[33] E. Flanagan, Phys. Rev. D **48**, 2389 (1993).
[34] B. Allen and J. Romano, Phys. Rev. D **59**, 102001 (1999).

[35] B. Allen and R. Brustein, Phys. Rev. D **55**, 3260 (1997).
[36] C. Ungarelli and A. Vecchio, gr-c/9911104.
[37] C. Copi *et al.*, Phys. Rev. Lett. **75**, 3981 (1995).
[38] R. Brustein, M. Gasperini, and G. Veneziano, Phys. Rev. D **55**, 3882 (1997).
[39] M. Gasperini, Phys. Rev. D **56**, 4815 (1997).
[40] M. Gasperini, hep-th/9607146.
[41] A. Buonanno, M. Lemoine, and K. A. Olive, Phys. Rev. D **62**, 083513 (2000).